Synthesis of N$_3^-$/SCN$^-$ bridged polynuclear complexes of nickel(II) using *N*,*N*,*N*′-trimethylethane-1,2-diamine as a blocking ligand: low temperature magnetic study and single crystal structure of [Ni($\mu_{1,1}$-N$_3$)($\mu_{1,3}$-N$_3$)(*N*,*N*,*N*′-Me$_3$en)]$_n$

Montserrat Monfort,*[a] Inmaculada Resino,[a] Joan Ribas,[a] Xavier Solans[b] and Mercé Font-Bardia[b]

[a] *Departament de Química Inorgànica, Universitat de Barcelona, Martí i Franqués 1-11, 08028 Barcelona, Spain. E-mail: montserrat.monfort@qi.ub.es; Fax: +34 93 490 77 25*
[b] *Departament de Cristal·lografia i Mineralogia, Universitat de Barcelona, Martí i Franqués s/n, 08028 Barcelona, Spain*

Received (in Montpellier, France) 2nd July 2001, Accepted 6th September 2001
First published as an Advance Article on the web

Seven new complexes of nickel(II), derived from azido, thiocyanato and nitrito bridging ligands and *N*,*N*,*N*′-trimethylethylenediamine (*N*,*N*,*N*′-Me$_3$en) as blocking ligand, were synthesised and characterised; four of them are one-dimensional compounds: [Ni($\mu_{1,3}$-N$_3$)(*N*,*N*,*N*′-Me$_3$en)$_2$]$_n$(ClO$_4$)$_n$ **1**, [Ni($\mu_{1,3}$-N$_3$)(*N*,*N*,*N*′-Me$_3$en)$_2$]$_n$(PF$_6$)$_n$ **2**, [Ni$\mu_{1,1}$-N$_3$)($\mu_{1,3}$-N$_3$)(*N*,*N*,*N*′-Me$_3$en)]$_n$ **3**, [Ni(μ-SCN)$_2$(*N*,*N*,*N*′-Me$_3$en)]$_n$ **4**, and three mononuclear: [Ni(NCS)$_2$(*N*,*N*,*N*′-Me$_3$en)$_2$] **5**, [Ni(NO$_2$)(*N*,*N*,*N*′-Me$_3$en)$_2$]PF$_6$ **6**, [Ni(NO$_2$)$_2$(*N*,*N*,*N*′-Me$_3$en)] **7**. Crystal structures for **3** and **6** were determined by X-ray diffraction methods. Compound **3** may be described as a one-dimensional system with double azido bridging ligands alternately in end-on and end-to-end co-ordination modes. Compound **6** is a mononuclear complex in which a nitrito ligand acts as a chelate. The magnetic properties of all the compounds were studied by susceptibility measurements *vs.* temperature. The χ_M *vs.* T plots for **1** and **2** show the typical shape for moderate antiferromagnetic one-dimensional nickel(II) complexes, while global strong antiferromagnetic behaviour with a maximum at about 200 K is observed for **3** and **4** exhibits a very weak ferromagnetic interaction. Compounds **5**, **6**, and **7** follow the Curie law, typical behaviour of mononuclear Ni^{II} compounds. The superexchange parameter J for **1**, **2** and **4** was deduced from the spin Hamiltonian $-J\Sigma \boldsymbol{S}_i\boldsymbol{S}_{i+1}$ and from $-\Sigma(J_{AF}\boldsymbol{S}_{2i}\boldsymbol{S}_{2i+1}+J_F\boldsymbol{S}_{2i}\boldsymbol{S}_{2i-1})$ for **3**. J values for **1** and **2** are -15.5 and -16.6 cm^{-1}, respectively, $J_{AF}=-132$ cm^{-1} and $J_{FM}=99$ cm^{-1} for **3**, and 1.34 cm^{-1} for **4**.

In recent years the synthesis of polynuclear complexes with a variety of bridging ligands has been developed mainly due to the search for molecular magnets. In order to control the synthesis of such complexes, different ancillary ligands that block some sites over the metal ion have been used. These kinds of ligands seem to be of great importance for determining the nature of the obtained complexes. Using *N*,*N*,*N*′-Me$_3$en (*N*,*N*,*N*′-trimethylethylenediamine) as blocking ligand with diamagnetic metal ions, several mononuclear compounds with Pt^{II} and Ti^{IV},[1] as well as homo-[2] and heterometallic[3] dinuclear compounds have been reported. The chemistry related to paramagnetic centres has been developed with different metal ions of the first transition series.

In this work, we focused our attention on the synthesis of polynuclear compounds using *N*,*N*,*N*′-Me$_3$en, Ni^{II} ions and three different bridging ligands: azido (N$_3^-$), thiocyanato (SCN$^-$) and nitrito (NO$_2^-$) ions. The most common of these three is N$_3^-$, which also shows the strongest magnetic interaction. With Ni^{II} there is a great diversity of compounds such as dinuclear, trinuclear, 1D and 2D nets,[4] in which the azido ligand shows different co-ordination modes. The most common are the $\mu_{1,3}$-N$_3^-$ (end-to-end) and the $\mu_{1,1}$-N$_3^-$ (end-on), and it is not uncommon to find both co-ordination modes alternating in a compound. Usually, with the former the magnetic interaction is antiferromagnetic and for the latter ferromagnetic.[4] The other two bridging ligands are less common than azido. With thiocyanato there are only a few polynuclear complexes showing the end-to-end co-ordination mode[5] and a great number of mononuclear[6] compounds. The versatility with nitrito is greater due to its ability to co-ordinate with metal ions in a variety of different ways. Monodentate co-ordination may occur either through nitrogen, giving a nitro complex, or through oxygen, giving a nitrito complex; bidentate co-ordination is known to take place either by chelation or by bridging.[7] Therefore, it gives different kinds of complexes, such as mononuclear, dinuclear, trinuclear, pentanuclear, heptanuclear and 1D complexes.[6–8] Herein we report two new cationic complexes using N$_3^-$: one with ClO$_4^-$ (**1**) and the other with PF$_6^-$ (**2**) as the counteranion, and a neutral one (**3**) for which the structure was solved. When using SCN$^-$, a neutral one-dimensional complex **4** and a mononuclear complex **5**, similar to others reported in the literature, were obtained. Finally, different mononuclear compounds using NO$_2^-$ were synthesised: a mononuclear one with hexafluorophosphate (**6**) as a counteranion (whose structure was solved), and a neutral one (**7**).

Experimental

Syntheses

All reagents were purchased from Aldrich Company and used as supplied.

Caution! Azido complexes of metal ions and perchlorate salts of metal complexes with organic ligands are potentially explosive. Only a small amount of material should be prepared and it should be handled with care.

[Ni(μ$_{1,3}$-N$_3$)(*N*,*N*,*N*′-Me$_3$en)$_2$]$_n$(ClO$_4$)$_n$, 1. Complex **1** was synthesised by mixing an aqueous solution of nickel(II) perchlorate hexahydrate (0.73 g, 2 mmol) and *N*,*N*,*N*′-Me$_3$en (0.42 g, 4 mmol), followed by drop-by-drop addition of an aqueous solution of sodium azide (0.13 g, 2 mmol). The mixture was then filtered to remove any impurity. The resulting blue mixture was left to evaporate. After a few days a pale blue powder was obtained. Yield 0.55 g, 68%. (Found: C, 29.5; H, 6.8; N, 24.4%. $C_{10}H_{28}ClN_7NiO_4$ requires C, 29.8; H, 7.0; N, 24.3%.) IR: ν_{max}/cm^{-1} (N_3^-) 2111 vs, (ClO_4^-) 1100 vs, 625 vs.

[Ni(μ$_{1,3}$-N$_3$)(*N*,*N*,*N*′-Me$_3$en)$_2$]$_n$(PF$_6$)$_n$, 2. Complex **2** was prepared in the same way as compound **1** but using nickel nitrate hexahydrate (0.58 g, 2 mmol) instead of nickel perchlorate and adding an aqueous solution of ammonium hexafluorophosphate (0.4 g, 2.5 mmol) at the end. The resulting blue mixture was left to evaporate. After a few days a pale blue powder was obtained. Yield, 0.64 g, 71%. (Found: C, 26.5; H, 6.0; N, 21.8%. $C_{10}H_{28}F_6N_7NiP$ requires C, 26.7; H, 6.3; N, 21.8%.) IR: ν_{max}/cm^{-1} (N_3^-) 2117 vs, (PF_6^-) 840 vs, 545 vs.

[Ni(μ$_{1,1}$-N$_3$)(μ$_{1,3}$-N$_3$)(*N*,*N*,*N*′-Me$_3$en)]$_n$, 3. Complex **3** was prepared as compound **2** but changing the quantities of the starting reagents and mixing the aqueous solution with acetonitrile: nickel(II) nitrate hexahydrate (0.58 g, 2 mmol), *N*,*N*,*N*′-Me$_3$en (0.21 g, 2 mmol) and sodium azide (0.26 g, 4 mmol). The green solution was filtered to remove any impurity and left to slowly evaporate. After two weeks green crystals suitable for X-ray determination were obtained. Yield 0.42 g, 82%. (Found: C, 24.7; H, 5.8; N, 45.9%. $C_5H_{14}N_8Ni$ requires C, 24.6; H, 5.8; N, 45.9%.) IR: ν_{max}/cm^{-1} (N_3^-) 2095 vs, 2058 vs.

[Ni(μ-SCN)$_2$(*N*,*N*,*N*′-Me$_3$en)]$_n$, 4. Complex **4** was prepared as compound **3**, but replacing sodium azide by ammonium thiocyanate (0.30 g, 4 mmol). The green solution was filtered to remove impurities and left to evaporate. After some weeks, a green crystalline powder was obtained. Yield 0.29 g, 52%. (Found: C, 30.4; H, 5.4; N, 20.1; S, 23.1%. $C_7H_{14}N_4NiS_2$ requires C, 30.4; H, 5.1; N, 20.3; S, 23.2%.) IR: ν_{max}/cm^{-1} (SCN^-) 2112 s, 787 w, and 470 w

[Ni(NCS)$_2$(*N*,*N*,*N*′-Me$_3$en)$_2$], 5. Complex **5** was prepared as compound **1**, using ammonium thiocyanate (0.15 g, 2 mmol) instead of sodium azide, in order to obtain a polynuclear compound, but only a mononuclear one was obtained. The resulting solution was purple–blue, and after several days, purple crystals were obtained. Yield 0.35 g, 47%. (Found: C, 38.0; H, 7.3; N, 22.2; S, 16.8%. $C_{12}H_{28}N_6NiS_2$ requires C, 38.1; H, 7.5; N, 22.2; S, 16.9%.) IR: ν_{max}/cm^{-1} (SCN^-) 2098 s 2082 s, 780 w, 475 w.

[Ni(NO$_2$)(*N*,*N*,*N*′-Me$_3$en)$_2$]PF$_6$, 6. Complex **6** was synthesised as **2**, using sodium nitrite (0.15 g, 2 mmol) instead of sodium azide. The resulting mixture was then filtered to remove any impurity. Blue crystals suitable for X-ray determination were obtained after a few days of evaporation. Yield 0.66 g, 73%. (Found: C, 26.3; H, 6.2; N, 15.5%. $C_{10}H_{28}F_6N_5NiO_2P$ requires C, 26.5; H, 6.2; N, 15.5%.) IR: ν_{max}/cm^{-1}(NO_2^-) 1288 w, 1235 w, 1225 w, (PF_6^-) 846 vs, 550 vs.

[Ni(NO$_2$)$_2$(*N*,*N*,*N*′-Me$_3$en)], 7. Complex **7** was synthesised as **3**, but adding drop-by-drop an aqueous solution of sodium nitrite (0.30 g, 4 mmol) instead of sodium azide. The resulting mixture was then filtered to remove any impurity. A dark blue crystalline powder was obtained after a few days. Yield 0.39 g, 77%. (Found: C, 29.4; H, 6.9; N, 16.8%. $C_5H_{14}N_4NiO_4$ requires C, 29.5; H, 6.9; N, 17.1%.) IR: ν_{max}/cm^{-1} (NO_2^-) 1298 w, 1287 w, 1215 w.

Spectral and magnetic measurements

Infrared spectra (400–4000 cm^{-1}) were recorded from KBr pellets on a Nicolet 520 FTIR spectrophotometer. Magnetic measurements were carried out with a pendulum-type magnetometer (MANICS DSM8) equipped with a helium continuous-flow cryostat working in the temperature range 300–4 K, and a Brucker B-E15 electromagnet. The magnetic field was approximately 1.5 T. Diamagnetic corrections were estimated from Pascal tables.

Crystal data collection and refinement

Crystallographic data for **3** and **6** were obtained on an Enraf–Nonius CAD4 diffractometer, with graphite monochromated Mo-Kα radiation ($\lambda = 0.71069$ Å) and the $\omega/2\theta$ scan technique, and appear in Table 1. Corrections were made for Lorentz polarisation but not for absorption. The structures were solved by direct methods, using the SHELXS97 computer program[9] and refined by a full-matrix least-squares method, using the SHELXL97 computer program.[10] The function minimised was $\Sigma w||F_o|^2 - |F_c|^2|^2$, where $w = [\sigma^2(F_o^2) + (k_1P)^2 + k_2P]^{-1}$ and where $k_1 = 0.0568(3)$ and $k_2 = 0(3)$ for **3** and $k_1 = 0.0717(3)$ and $k_2 = 0.0256(3)$ for **6**. f, f' and f'' were taken from the literature.[11] For **3**, the extinction coefficient was 0.0036(11) and 0.0101(11) for **6**. For **3**, 11 H atoms were located from a difference synthesis and refined with an overall isotropic temperature factor while 3 H atoms were computed and refined with an overall isotropic temperature factor, using a riding model. For **6**, 2 H atoms were located from a difference synthesis and refined with an overall isotropic temperature factor and 26 H atoms were computed and refined with an overall isotropic temperature factor using a riding model. The chirality of structure **6** was defined from the Flack coefficient, which it is equal to 0.00 for the given results.[12] The crystallographic data, conditions retained for the intensity data collection, and some features of the structure refinements are listed in Table 1.

Table 1 Crystallographic data for **3** and **6**

	3	**6**
Empirical formula	$C_5H_{14}N_8Ni$	$C_{10}H_{28}F_6N_5NiO_2P$
M	244.95	454.05
T/K	293(2)	293(2)
Crystal system	Monoclinic	Orthorhombic
Space group	$P2_1/n$	$Pca2_1$
a/Å	7.132(4)	12.698(2)
b/Å	10.122(2)	10.1097(14)
c/Å	14.614(5)	15.698(5)
β/°	102.22(2)	90
U/Å^3	1031.1(7)	2015.2(8)
Z	4	4
μ(Mo-Kα)/mm^{-1}	1.859	1.108
Reflections collected	3137	5326
Independent reflections	2997	2811
Observed reflections	1688	2562
R(int)	0.015	0.022
R(F) observed	0.050	0.037
wR (all)	0.140	0.118

CCDC reference numbers 162464 and 162465. See http://www.rsc.org/suppdata/nj/b1/b105770g/ for crystallographic data in CIF or other electronic format.

Results and discussion

Description of the structure of $[Ni(\mu_{1,1}\text{-}N_3)(\mu_{1,3}\text{-}N_3)(N,N,N'\text{-}Me_3en)]_n$, 3

An ORTEP plot of the basic unit is shown in Fig. 1. The structure consists of neutral chains of nickel(II) linked by alternating double end-on and end-to-end azido bridge ligands along the *a* direction (Fig. 2). The nickel atoms are octahedrally co-ordinated: two sites of its co-ordination sphere are occupied by the blocking ligand, *N*,*N*,*N*′-Me$_3$en, and the other four by azido ligands. The azido ligands are linked with two neighbouring nickel ions. Therefore each nickel ion shows a distorted octahedral co-ordination. This compound shows two asymmetric centres over the two different double azido bridges, but structurally there is only one type of nickel(II). The two Ni–N distances for the diamine are different: 2.152(4) and 2.095(4) Å. The Ni–N lengths for the azido ligand in the end-on (EO) co-ordination mode are longer than in the end-to-end (EE) one: 2.136(3) and 2.130(3) Å for the former and 2.107(4) and 2.091(3) Å for the latter. The most important structural features are some of the angles in the double bridge, which are directly related to the magnetic coupling. The Ni–N–Ni angle in the EO mode is 100.52(13)° and lies in the range of all known $Ni(\mu_{1,1}\text{-}N_3)_2Ni$ angles.[4] The Ni–N–N angles in the EE mode are 129.6(3) and 129.9(3)°, and as above, lie in the range of other known $Ni(\mu_{1,3}\text{-}N_3)_2Ni$ angles.[4] The $Ni(\mu_{1,3}\text{-}N_3)_2Ni$ dihedral angle δ, also magnetically important, is in this compound 9.6°. The main distances and angles are listed in Table 2.

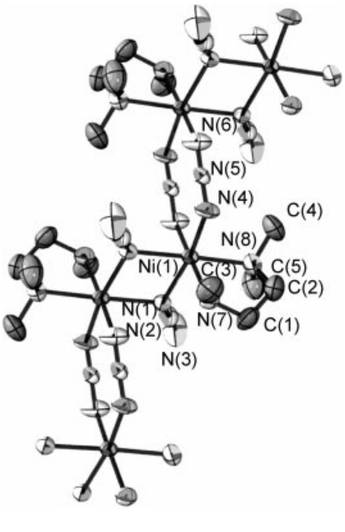

Fig. 1 ORTEP drawing and labeling scheme of $[Ni(\mu_{1,1}\text{-}N_3)(\mu_{1,3}\text{-}N_3)(N,N,N'\text{-}Me_3en)]_n$, **3**. Ellipsoids are at the 50% probability level.

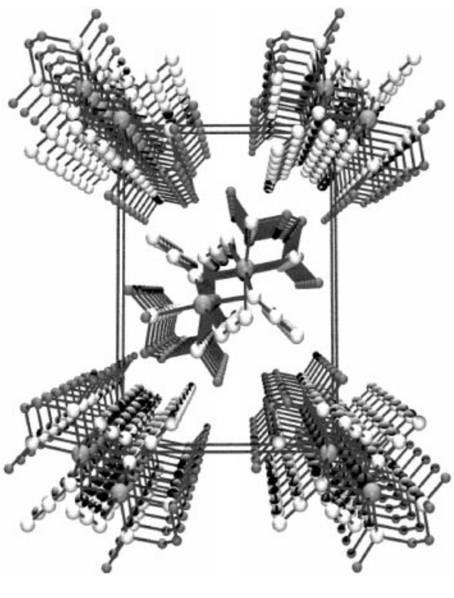

Fig. 2 View of the unit cell of $[Ni(\mu_{1,1}\text{-}N_3)(\mu_{1,3}\text{-}N_3)(N,N,N'\text{-}Me_3en)]_n$, **3**. The hydrogen atoms are omited for clarity.

Description of the structure of $[Ni(NO_2)(N,N,N'\text{-}Me_3en)_2](PF_6)$, 6

The structure of **6** is shown in Fig. 3. It consists of octahedrally co-ordinated nickel(II) atoms in which two blocking ligands and one nitrito ligand occupy the co-ordination sites. This nitrito ligand acts as a chelate, co-ordinating two of the sites of the Ni^{II} with its oxygen atoms; the O–Ni–O angle is 57.3(2)°. The other four positions of the nickel ion are linked to nitrogen atoms of the diamine. The four Ni–N distances are different: the smallest is 2.110(3) Å [Ni(1)–N(2)] and the biggest is 2.166(4) Å [Ni(1)–N(4)]. The two Ni–O distances are also different: 2.162(4) [Ni(1)–O(1)] and 2.192(2) Å [Ni(1)–O(2)]. The N–Ni–N angles in *cis* position are far from 90° because of the nitrito ligand chelation: the smallest is the N(3)–Ni–N(4) angle [83.32(13)°], and the biggest is N(1)–Ni(1)–N(4) [108.95(13)°]. Each one of these units corresponds to one hexafluorophosphate anion. Main distances and angles are listed in Table 3.

Table 2 Selected bond lengths (Å) and angles (°) for $[Ni(\mu_{1,1}\text{-}N_3)(\mu_{1,3}\text{-}N_3)(N,N,N'\text{-}Me_3en)]_n$, **3**[a]

Ni(1)–N(1)	2.130(3)	Ni(1)–N(8)	2.152(4)
Ni(1)–N(1)#2	2.136(3)	N(1)–N(2)	1.188(5)
Ni(1)–N(4)	2.091(3)	N(2)–N(3)	1.145(5)
Ni(1)–N(6)#1	2.107(4)	N(4)–N(5)	1.164(4)
Ni(1)–N(7)	2.095(4)	N(5)–N(6)	1.159(4)
N(1)–Ni(1)–N(4)	168.07(14)	N(4)–Ni(1)–N(7)	91.87(14)
N(1)–Ni(1)–N(6)#1	88.40(14)	N(4)–Ni(1)–N(8)	90.5(2)
N(1)–Ni(1)–N(7)	85.91(14)	N(6)#1–Ni(1)–N(7)	171.48(14)
N(1)–Ni(1)–N(8)	100.89(14)	N(6)#1–Ni(1)–N(8)	91.3(2)
N(1)–Ni(1)–N(1)#2	79.48(13)	N(7)–Ni(1)–N(8)	83.5(2)
N(1)#2–Ni(1)–N(4)	88.94(14)	Ni(1)–N(1)–Ni(1)#2	100.52(13)
N(1)#2–Ni(1)–N(6)#1	92.2(3)	N(3)–N(2)–N(1)	179.0(6)
N(1)#2–Ni(1)–N(7)	92.98(14)	N(5)–N(4)–Ni(1)	129.9(3)
N(1)#2–Ni(1)–N(8)	176.45(13)	N(5)–N(6)–Ni(1)#1	129.6(3)
N(4)–Ni(1)–N(6)#1	95.0(2)	N(6)–N(5)–N(4)	175.9(4)

[a] Symmetry transformations are: $\#1 = 2 - x, -y, 2 - z$ and $\#2 = 1 - x, -y, 2 - z$.

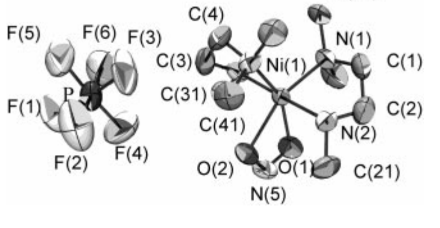

Fig. 3 ORTEP drawing of $[Ni(NO_2)(N,N,N'\text{-}Me_3en)_2]PF_6$, **6**, and the atom labeling scheme. Ellipsoids are at the 50% probability level.

Table 3 Selected bond lengths (Å) and angles (°) for $[Ni(NO_2)(N,N,N'\text{-}Me_3en)_2]PF_6$, **6**

Ni–N(1)	2.146(3)	Ni–O(1)	2.162(4)
Ni–N(2)	2.110(3)	Ni–O(2)	2.192(2)
Ni–N(3)	2.116(3)	N(5)–O(1)	1.246(5)
Ni–N(4)	2.166(4)	N(5)–O(2)	1.256(6)
N(4)–Ni–N(1)	108.95(13)	N(2)–Ni–O(2)	92.66(13)
N(4)–Ni–O(1)	154.39(13)	N(3)–Ni–N(1)	95.31(13)
N(1)–Ni–O(1)	96.66(14)	N(3)–Ni–N(4)	83.32(13)
O(1)–Ni–O(2)	57.3(2)	N(3)–Ni–O(1)	94.54(14)
N(2)–Ni–N(3)	177.5(2)	N(3)–Ni–O(2)	88.89(11)
N(2)–Ni–N(1)	84.1(2)	N(4)–Ni–O(2)	97.1(2)
N(2)–Ni–N(4)	94.6(2)	N(1)–Ni–O(2)	154.0(2)
N(2)–Ni–O(1)	87.90(14)		

Magnetic properties

The variable temperature magnetic susceptibility data were recorded for all compounds between 300–4 K. Compounds **1**, **2** and **3** show an antiferromagnetic interaction between the metal ions and compound **4** shows a ferromagnetic interaction. Compounds **5**, **6** and **7** follow the Curie law, showing the typical behaviour of mononuclear compounds. The molar susceptibilities for **1** and **2** are plotted in Fig. 4. For both compounds, the molar susceptibility value (4.3 and 4.5×10^{-3} cm^3 mol^{-1} for **1** and **2** at room temperature, respectively) increases when the temperature decreases until they reach a maximum value (1.6×10^{-2} cm^3 mol^{-1} at 28 K for **1** and 1.56×10^{-2} cm^3 mol^{-1} at 30 K for **2**). Then they decrease continuously to 1.03 and 1.05×10^{-2} cm^3 mol^{-1} for **1** and **2** at 4 K, respectively. The antiferromagnetic behaviour suggests that the azido bridge is in the end-to-end co-ordination mode in both cases. The IR study confirms this supposition: the two different modes of the azido ligand (end-to-end and end-on) show a very strong band in the range 2150–2050 cm^{-1}, which corresponds to v_{as}. According to the literature,[13] the band attributable to the end-to-end mode appears at higher frequencies (close to 2100 cm^{-1}) than those corresponding to the end-on co-ordination mode (close to 2060 cm^{-1}). In compounds **1** and **2** this band appears at 2115 and 2117 cm^{-1}, respectively.

The elemental analysis of both compounds fits well with the ratio Ni^{2+} : amines : N_3^- : X (where $X = ClO_4^-$ or PF_6^-) being 1 : 2 : 1 : 1. This ratio can correspond to a dinuclear complex with a double azido bridge or to a monodimensional complex with a single azido bridge between two nickel ions. The experimental magnetic data have been fitted with the appropriate expression, taking into account the two possibilities (dinuclear or one-dimensional). With the expression for an antiferromagnetic dinuclear complex $S = 1$, the fit obtained was very poor. For this reason we assume that the complexes are not dinuclear ones. In contrast, using the expression for an antiferromagnetic one-dimensional $S = 1$ complex, the fit obtained was good. In this case, the general spin Hamiltonian to describe the magnetic properties of isotropic Ni$^{\text{II}}$ chains, taking into account the single-ion terms and the interactions between the nearest neighbour centre was used:

$$H = \Sigma(\beta \boldsymbol{S}_i g_i H - J \boldsymbol{S}_i \boldsymbol{S}_i) \qquad (1)$$

The terms corresponding to the anisotropic and antisymmetric exchange have not been considered because these effects are relevant only at very low temperatures. For systems of this kind, isotropic 1-D $S = 1$, the temperature dependence of the susceptibility extrapolated from calculations performed on ring systems of increasing length has been given by Weng.[14] The Weng equation is valid only for antiferromagnetic coupling. A good fit is possible only down to a temperature near the maximum of χ_M because neither zero-field splitting nor the Haldane gap effect[15] is taken into account in the Weng expression. The J values were obtained by minimising the function $R = \Sigma(\chi_M^{calc} - \chi_M^{obs})^2/\Sigma(\chi_M^{obs})^2$. The best fit parameters for **1** are: $J = -15.5$ cm^{-1}, $g = 2.32$ and $R = 3.2 \times 10^{-4}$. For **2** they are: $J = -16.6$ cm^{-1}, $g = 2.38$ and $R = 1.2 \times 10^{-4}$. The low values of R confirm that the compounds are 1D.

Compound **3** shows a strong antiferromagnetic behaviour, as can be seen in Fig. 5. χ_M is 3.2×10^{-3} cm^3 mol^{-1} at room temperature. Then, χ_M increases on cooling, showing a maximum at about 200 K and after that decreases continuously until it reaches a minimum at 1.26×10^{-2} cm^3 mol^{-1} at 20 K. Below 20 K, χ_M tends to infinity as T tends to zero. In order to fit this behaviour, we used a theoretical model based on the calculation of the properties of finite rings of increasing size,[16] for Heisenberg ferro-antiferromagnetic $S = 1$ chains, the Hamiltonian of which is:

$$H = -\sum_{i=1}^{N-1} (J_{AF} \boldsymbol{S}_{2i} > \boldsymbol{S}_{2i+1} + J_{FM} \boldsymbol{S}_{2i} \boldsymbol{S}_{2i-1})$$

where N is the number of spins pairs, J_{AF} and J_{FM} are the nearest neighbour antiferro- and ferromagnetic exchange interactions. Using the analytical expression deduced by El

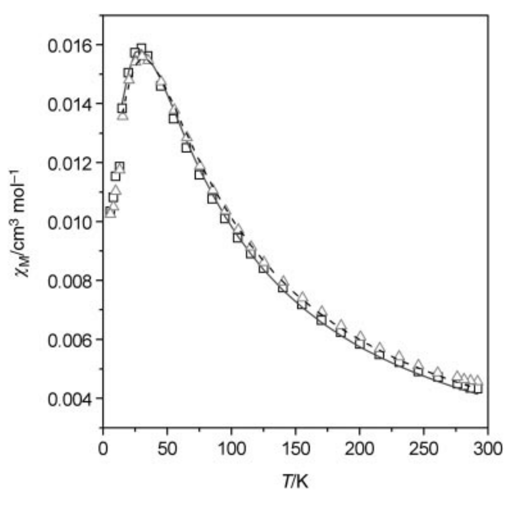

Fig. 4 Plot of magnetic susceptibility versus temperature for $[Ni(\mu_{1,3}\text{-}N_3)(N,N,N'\text{-}Me_3en)_2]_n(ClO_4)_n$ **1** (□) and $[Ni(\mu_{1,3}\text{-}N_3)(N,N,N'\text{-}Me_3en)_2]_n(PF_6)_n$ **2** (△). Solid line represents the best theoretical fit (see text).

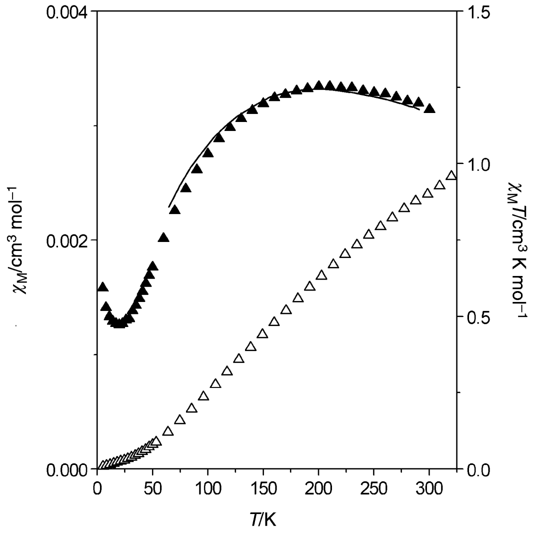

Fig. 5 Plots of observed χ_M (△) and $\chi_M T$ (▲) *versusT* for $[Ni(\mu_{1,1}\text{-}N_3)(\mu_{1,3}\text{-}N_3)(N,N,N'\text{-}Me_3en)]_n$, **3**. Solid line represents the best theoretical fit (see text).

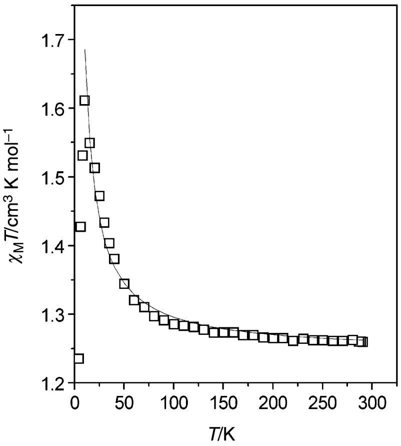

Fig. 6 Plot of observed $\chi_M T$ *versus* T for [Ni(μ-SCN)$_2$(*N*,*N*,*N*′-Me$_3$en)]$_n$, **4**. Solid line shows the best fit obtained.

Fallah *et al.*,[16] which is valid for $kT/|J_{AF}| \geq 0.22$, the calculated magnetic susceptibility of the infinite chain is in good agreement with the data. Below this value, there are other phenomena such as ZFS or interactions between different chains that lead to deviations from the data. So, the best results of this fit are: $J_{AF} = -132$ cm^{-1}, $J_{FM} = 99$ cm^{-1}, $g = 2.35$ and $R = 1.6 \times 10^{-4}$. It is important to note that the antiferromagnetic interaction is related to the temperature at which the maximum appears and the ferromagnetic interaction is related to the pendant of the curve of χ_M before this maximum; so with this kind of compound in which J_{AF} is large and the maximum is settled at high temperatures, the value of J_{FM} shows less precision.

Compound **4** shows a weak ferromagnetism. Fig. 6 is the plot of $\chi_M T$ *vs.* T in the range 300–4 K. At 300 K, $\chi_M T$ is 1.26 cm^3 K mol^{-1}, showing a maximum at 10 K (1.61 cm^3 K mol^{-1}). From the elemental analysis the Ni^{II} : amine : SCN$^-$ ratio for this compound is 1 : 1 : 2, so two co-ordination sites of the Ni^{II} are occupied by the N of the diamine and the other four by the SCN$^-$ acting as double bridges between two Ni ions. Thus, we propose a one-dimensional structure for this compound with a double thiocyanate bridge. The experimental data was fitted by the empirical relation proposed by de Neef[17] for $S = 1$ ferromagnetic chains. The minimisation of the agreement factor leads to $J = 1.34$ cm^{-1}, $g = 2.23$ and $R = 3.2 \times 10^{-4}$. The interaction is weak as in other compounds reported in the literature.[5]

Magnetostructural correlations

For monodimensional compounds with only one end-to-end azido bridge the most significant structural parameters are the Ni–N$_{azide}$–Ni torsion angle and the Ni–N–N angle. The best antiferromagnetic coupling appears when the torsion angle is 0° and decreases gradually thereafter as the torsion angle increases to 90°. The maximum coupling is expected for a Ni–N–N angle of 108° while for greater values the antiferromagnetic interaction must decrease. In the same fashion in the *cis* complexes, the torsion angles are greater than in *trans* complexes, thus, creating, lower antiferromagnetic coupling. For compounds **1** and **2**, taking into account the absence of crystal structure, we can only postulate that the number of substituents on the N atoms of the diamine creates a steric impediment and forces a large torsion angle or a *cis* arrangement, as in other substituted diamines (2-aminoethylpyridine and 1,2-diamino-2-methylpropane).[4] This supposition is in agreement with the small values of the J parameter, comparable with those of compounds having a *cis* arrangement, and smaller than those obtained for the compounds with *trans* geometry.

For compound **3**, with regard to the antiferromagnetic part (EE azido bridges), previous studies[4] show that the value of the superexchange coupling depends mainly, when the two pseudohalides are parallel, on the dihedral angel δ. J_{AF} has maximum values for dihedral angles close to 0°, and deviation from the planar geometry reduces the overlap between magnetic orbitals. The J_{AF} value diminishes and reaches a value of 0 when the value of the dihedral angle is close to 60°. Taking into account these considerations, the small δ value for compound **3** (9.6°) agrees well with the large experimental J_{AF}. In addition, the results compare well with those reported in the literature.[4] Looking to the ferromagnetic part (EO azido bridges), the recent magneto-structural correlations by Ruiz *et al.*[18] for azido-bridged Ni(II) complexes show that the most important parameter in the ferromagnetic coupling is the Ni–N$_{azide}$–Ni angle, which predicts a narrow range for the bond angle (± 8°) around 104° within which minor J differences should be expected.

Compound **4** shows weak ferromagnetic coupling like all those reported in the literature. This can be attributed to the rectangular geometry forced by the SCN$^-$ group. Previous studies[5c,d] have demonstrated that the more rectangular the geometry, the greater the orthogonality of the orbitals and, thus, the greater the possibility of ferromagnetic coupling.

Acknowledgements

This work was undertaken with the financial support of CICYT BQU2000-0791. I. R. thanks Ministerio de Educación y Cultura for a doctoral FPI fellowship. We are very grateful to Dr Nuria Clos for technical assistance with the magnetic measurements.

References

1 (*a*) K. Yokoho, K. Matsumoto, S. Ooi and H. Kuroya, *Bull. Chem. Soc. Jpn.*, 1976, **49**, 1864; (*b*) K. Matsumoto and S. Ooi, *Z. Kristallogr.*, 1979, **150**, 139; (*c*) S. R. Drake, K. P. Sanderson, M. B. Hursthouse and K. M. A. Malik, *Polyhedron*, 1994, **13**, 181.

2 (*a*) T. Laube, J. D. Dunitz and D. Seebach, *Helv. Chim. Acta*, 1985, **68**, 1373; (*b*) N. Feeder, R. Snaith and A. E. H. Wheatley, *Eur. J. Inorg. Chem.*, 1998, 879.

3 J. Ribas, C. Diaz, R. Costa, J. Tercero, X. Solans, M. Font-Bardia and H. Stoeckli-Evans, *Inorg. Chem.*, 1998, **37**, 233.

4 J. Ribas, A. Escuer, M. Monfort, R. Vicente, R. Cortés, L. Lezama and T. Rojo, *Coord. Chem. Rev.*, 1999, **193–195**, 1027.

5 (*a*) A. E. Shvelashvili, *Acta Crystallogr., Sect. A*, 1996, **21**, 153; (*b*) U. Turpeinen and M. Ahlgren, *Finn. Chem. Lett.*, 1977, 7; (*c*) A. P. Ginsberg, R. L. Martin, R. W. Brookes and R. C. Sherwood, *Inorg. Chem.*, 1972, **11**, 2884; (*d*) M. Monfort, J. Ribas and X. Solans, *Inorg. Chem.*, 1994, **33**, 4271; (*e*) M. Monfort, C. Bastos, C. Díaz, J. Ribas and X. Solans, *Inorg. Chim. Acta*, 1994, **218**, 185; (*f*) A. Escuer, S. B. Kumar, F. Mautner and R. Vicente, *Inorg. Chim. Acta*, 1998, **269**, 313; (*g*) R. Vicente, A. Escuer, J. Ribas, M. S. El Fallah, X. Solans and M. Font-Bardia, *J. Chem. Soc., Dalton Trans.*, 1994, 259; (*h*) M. D. Duggan and D. N. Hendrickson, *Inorg. Chem.*, 1974, **13**, 2929; (*i*) T. Rojo, R. Cortes, L. Lezama, M. I. Airrortua, K. Urtiaga and G. Villeneuve, *J. Chem. Soc., Dalton Trans.*, 1991, 1779.

6 (*a*) A. B. P. Lever, I. M. Walker, P. J. McCarthy, K. B. Mertes, A. Jircitano and R. Sheldon, *Inorg. Chem.*, 1983, **22**, 2252; (*b*) B. W. Brown and E. C. Lingafelter, *Acta Crystallogr.*, 1963, **16**, 753; (*c*) A. K. Mukherjee, M. Mukherjee, A. J. Welch, A. Ghosh, G. De and N. R. Chauduri, *J. Chem. Soc., Dalton Trans.*, 1987, 997; (*d*) U. Turpeinen, M. Ahlgren and R. Hamalainen, *Finn. Chem. Lett.*, 1980, 11; (*e*) M. A. Porai-Koshits, *Acta Crystallogr., Sect. A*, 1966, **21**, 149; (*f*) A. E. Shvelashvili, M. A. Porai-Koshits, A. I. Kvitashvili, B. M. Shchedrin and M. G. Tavberidze, *Zh. Strukt. Khim.*, 1974, **15**, 313; (*g*) C. Pariya, A. Ghosh, N. R. Chauduri, S. Ghosh, M. Mukherjee and A. K. Mukherjee, *Polyhedron*, 1996, **15**, 1643.

7 I. Resino, M. Monfort, J. Ribas, M. Font-Bardia and X. Solans, *Polyhedron*, 2000, **19**, 225 and references therein

8 (*a*) G. J. Mcdougall and R. D. Hancock, *J. Chem. Soc.*, 1980, 654; (*b*) A. J. Finney, M. A. Hitchman, C. L. Raston, G. L. Rowbottom and A. H. White, *Aust. J. Chem.*, 1981, **34**, 2047; (*c*) A. Gleizes, A. Meyer, M. A. Hitchman and O. Kahn, *Inorg. Chem.*, 1982, **21**, 2257; (*d*) I. M. Vezzosi, A. Benedetti, M. Saladini, L. P. Battagliaand and A. B. Corradi, *Inorg. Chim. Acta*, 1985, **97**, 195; (*e*) A. Pajunen, *Suom. Kemistil. B.*, 1968, **41**, 232; (*f*) M. J. Goldberg and R. E. Marsh, *Acta Crystallogr., Sect., B*, 1979, **35**, 960; (*g*) J. Ribas, M. Monfort, J. Vilana, X. Solans and M. Font-Altaba, *Transition Met. Chem.*, 1985, **10**, 340; (*h*) J. Ribas, M. Monfort, C. Diaz, M. Font-Altaba and X. Solans, *J. Crystal. Spectrosc. Res*, 1987, **17**, 303; (*i*) S. F. Palopoli, S. J. Geib, A. L. Rheingold and T. B. Brill, *Inorg. Chem.*, 1988, **27**, 2963; (*j*) D. M. Liebig and J. H. Robertson, *J. Chem. Soc.*, 1965, 5081; (*k*) L. K. Minacheva, M. A. Porai-Koshits and A. S. Antsyshkina, *Zh. Strukt. Khim.*, 1969, **10**, 79; (*l*) M. G. B. Drew, D. M. L. Goodgame, M. A. Hitchamn and D. Rogers, *Chem. Commun.*, 1965, 476; (*m*) L. K. Minacheva, A. S. Antsyshkina, M. A. Porai-Koshits and A. E. Shvelashvili, *Zh. Strukt. Khim.*, 1970, **11**, 936; (*n*) E. Turpeinen, *Suom. Kemistil. B.*, 1973, **46**, 208; (*o*) J. A. Cook, M. G. B. Drew and D. A. Rice, *J. Chem. Soc., Dalton Trans.*, 1975, 1973; (*p*) M. G. B. Drew, D. M. L. Goodgame, M. A. Hitchamn and D. Rogers, *Proc. Chem. Soc. (London)*, 1964, 363; (*q*) L. N. Swink and M. Atoji, *Acta Crystallogr.*, 1960, **13**, 639; (*r*) J. K. Korp, I. Bernal, R. A. Palmer and J. C. Robinson, *Acta Crystallogr., Sect. B*, 1980, **36**, 560; (*s*) S. Koner, A. Ghosh, C. Pariya, D. Das, H. Kikiuchi, I. Okamoto and R. Ikeda, *J. Mol. Struct.*, 1995, **345**, 265.

9 G. M. Sheldrick, SHELXS, Computer Program for Crystal Structure Determination, University of Göttingen, Germany, 1997.

10 G. M. Sheldrick, SHELXL, Computer Program for Crystal Structure Determination, University of Göttingen, Germany, 1997.

11 *International Tables for X-ray Crystallography*, Kynoch Press, Birmingham, England, 1974 , vol. IV, pp. 99.110 and 149.

12 H. D. Flack, *Acta. Crystallogr., Sect. A*, 1983, **39**, 876.

13 R. Cortés, M. Drillon, X. Solans, L. Lezama and T. Rojo, *Inorg. Chem.*, 1997, **36**, 677.

14 C. Y. Weng, Ph.D. Thesis, Carnegie Institute of Technology, USA, 1968.

15 (*a*) F. D. M. Haldane, *Phys. Rev. Lett.*, 1983, **50**, 1153; (*b*) F. D. M. Haldane, *Phys. Lett. A*, 1983, **93**, 464; (*c*) J. P. Renard, M. Verdaguer, L. P. Regnault, W. A. C. Erkelens, J. Rossat-Mignon and W. G. Stirling, *Europhys. Lett.*, 1987, **3**, 945; (*d*) J. P. Renard, M. Verdaguer, L. P. Regnault, W. A. C. Erkelens, J. Rossat-Mignon, J. Ribas, W. J. Stirling and C. J. Vettier, *Appl. Phys.*, 1988, **63**, 3538.

16 A. Escuer, R. Vicente, M. S. El Fallah, S. B. Kumar, F. A. Mautner and D. Gatteschi, *J. Chem. Soc., Dalton. Trans.*, 1998, 3905.

17 T. de Neef, Ph.D. Thesis, University of Technology, Eindhoven, The Netherlands, 1975.

18 E. Ruiz, J. Cano, S. Alvarez and P. Alemany, *J. Am. Chem. Soc.*, 1998, **120**, 11 122.